Statistical process control and mapping accuracy standards applied to aerial surveys[1]

Controle estatístico de processo e padrão de exatidão cartográfico aplicado a aerolevantamento

Vinícius Bitencourt Campos Calou[2]*, Adunias dos Santos Teixeira[3], José Adriano da Silva[4], Márcio Regys Rabelo de Oliveira[5] and Ícaro Vasconcelos do Nascimento[6]

ABSTRACT - Remotely piloted aircraft (RPA) are established in the market as a powerful tool for acquiring aerial images and facilitating mapping for various purposes. The aim of this study was to evaluate the quality of processes originating from the generation of georeferenced digital products employing a differing number of ground control points (GCP), using Statistical Process Control (SPC) and Mapping Accuracy Standards (MAS) in an orthomosaic produced with images from an RPA. A multirotor RPA was used to acquire aerial images over an area of 2 hectares. An orthomosaic was later generated using the PhotoScan software, and georeferenced with eight, five and three GCP (ground control points). Positioning errors were submitted to SPC to evaluate the quality of each process, and the orthomosaics were qualified by MAS. The results are promising, in view of the positioning errors of less than 0.1 m in the generated orthomosaics, which are classified as Mapping Accuracy Standards class 'A'. Statistical Process Control showed acceptable levels of error, indicating the high accuracy of surveys of this nature. The precision obtained when mapping shows that aerial images obtained by means of RPA can be used in topographic surveys as long as error standards and process control are observed, attesting to the quality of the results.

Keywords: Topography. PhotoScan. Drone. Structure from motion. RPA.

RESUMO - Os *remotely piloted aircrafts* - RPAs, estão firmados no mercado como poderosa ferramenta de aquisição de imagens aéreas, facilitando os mapeamentos para diversos fins. Assim, objetivou-se avaliar a qualidade dos processos a partir da geração de produtos digitais georreferenciados com diferentes quantidades de pontos de controle (GCPs), utilizando Controle Estatístico de Processos (CEP) e Padrão de Exatidão Cartográfico (MAS) em ortomosaico produzido com imagens de RPA. Foi utilizado um RPA multirotor para aquisição de imagens aéreas em área de 2 hectares. Posteriormente foi gerado ortomosaico por meio do software PhotoScan, georreferenciado com oito, cinco e três GCPs (Pontos de controles). Os erros de posicionamento foram submetidos ao CEP para avaliar a qualidade dos processos e os ortomosaicos foram qualificados pelo MAS. Os resultados são promissores, tendo em vista os erros de posicionamento menores que 0,1 m nos ortomosaicos gerados, classificados como padrão "A" de Exatidão Cartográfica. Os Controles Estatísticos de Processos demonstraram níveis aceitáveis de erros, indicando grande acurácia para levantamentos desta natureza. As elevadas precisões obtidas nos mapeamentos indicam que imagens aéreas obtidas por meio de RPAs podem ser utilizadas em levantamentos topográficos, contanto que se respeitem os padrões de erros e controle de processos, atestando a qualidade dos resultados.

Palavras-chave: Topografia. PhotoScan. Drone. Structure from motion. RPA.

INTRODUCTION

Remotely piloted aircraft (RPA) are used for monitoring cultivated areas to identify pests, diseases and invasive plants, nutritional deficiency in agricultural crops and water deficit, and to aid in crop forecasting, monitoring soil erosion and estimating crop biomass (ALSALAM *et al.*, 2017; ANUROGO *et al.*, 2017; CALOU *et al.*, 2019; FLYNN; CHAPRA, 2014; TSOUROS; BIBI; SARIGIANNIDIS, 2019).

The accuracy of this mapping process is of paramount importance for aerial surveys, attesting to imaging capability by means of statistical processes (AGÜERA-VEGA; CARVAJAL-RAMÍREZ; MARTÍNEZ-CARRICONDO, 2017; HUGENHOLTZ *et al.*, 2013 LIMA *et al.*, 2018; SALVINI *et al.*, 2018).

In this setting, Bachmann *et al.* (2013) evaluated the accuracy of a system for acquiring geographic data from an RPA employing 40 GCP. The mean error obtained in the orthomosaic was 30 cm; however, the resolution of the camera (1.5 megapixels) may have prevented further refinement of the results.

Gómez-Candón, de Castro and López-Granados (2014) sought to assess the accuracy of orthophotos taken at different flying altitudes and with a differing number of GCP for use in georeferencing. The results showed no significant differences in geometric accuracy between flights carried out at different altitudes (30, 60 and 100 m). The authors also demonstrated that the increase in GCP did not result in any significant increase in the precision of the processed model.

Siebert and Teizer (2014) carried out tests to estimate the accuracy of models generated from processing an orthomosaic using the PhotoScan software, employing an RPA at an altitude of 50 metres relative to ground level, where they achieved mean horizontal errors of 0.6 cm with nine GPC.

Zanetti, Gripp Junior and Santos (2017) point out that both the number and arrangement of GCP are extremely important, as they directly influence the quality of the generated product, considerably increasing the accuracy of the maps.

Works of this nature notably seek to assess the level of accuracy of surveys at the expense of using a different number of control points and their distribution in the field, onboard sensors or different flying altitudes.

In Brazil, precision analysis of cartographic products and other processes is based on the application of Mapping Accuracy Standards, which include calculating the mean squared error (MSE) and the vertical tolerance (MICELI *et al.*, 2011; NORONHA *et al.*, 2011; SILVA *et al.*, 2013; TAKAHASHI *et al.*, 2012). According to Montgomery (2004), another factor is that Statistical Process Control (SPC) comprises a set of statistical techniques that are used to monitor and improve the various processes. The essence of SPC therefore is to monitor the inherent variation in a process, called the natural variation, and distinguish it from specific causes, which are generally identifiable.

In view of the above, the aims of this study were: 1) to assess the cartographic accuracy of the orthomosaic obtained from high spatial resolution aerial images, allowing these tools to be used in mapping; 2) to assess horizontal and vertical errors in the GNSS system (Global Navigation Satellite System) using a differing number of GCP so that they conform to control limits; and 3) to categorise the digital products generated from aerial images using Mapping Accuracy Standards and Statistical Process Control, and attest to the accuracy of the mapping.

MATERIAL AND METHODS

The work was carried out on a private area of two hectares in the rural sector of Itaitinga in the metropolitan region of Fortaleza, Ceará, located at 3°55'5.76" S and 38°30'28.80" W (Figure 1). The area has predominantly flat to gently undulating relief, with a mean altitude of 30 metres, native undergrowth and a sub-humid hot tropical climate, with an average rainfall of 1,416.4 mm yr^{-1} (FUNDAÇÃO CEARENSE DE METEOROLOGIA E RECURSOS HÍDRICOS, 2018).

A Phantom 2 remotely piloted aircraft (RPA) was used, manufactured by DJI Innovations. The Phantom line of RPA are categorised as multi-rotor vehicles (Quadrotor), with an approximate flight time of 15 minutes, a capacity of 5200 mAh and a voltage of 11.1v. Flight commands are carried out along the three axes, to move the RPA forward and backward (Pitch), right and left (Roll), and rotate it along its own axis to the right and left (Yaw). The RPA platform includes a built-in system, the Inertial Measurement Unit (IMU), providing altitude control through an inertial sensor and a barometric altimeter. The Compass system reads geomagnetic information with the aid of GPS (Global Position System) thereby increasing accuracy when calculating the position and height of the RPA. The Phantom also has a Zenmuse H3-3D camera stabiliser system (Gimbal), which improves the quality of the images or video obtained with the platform during flight. Mounted on the RPA was a GoPro Hero 4 Silver fish-eye RGB camera, with 12 megapixels and a focal length of 2.8 mm.

Figure 1 - Map of the study area in the district of Itaitinga, metropolitan region of Fortaleza, Ceará, Brazil
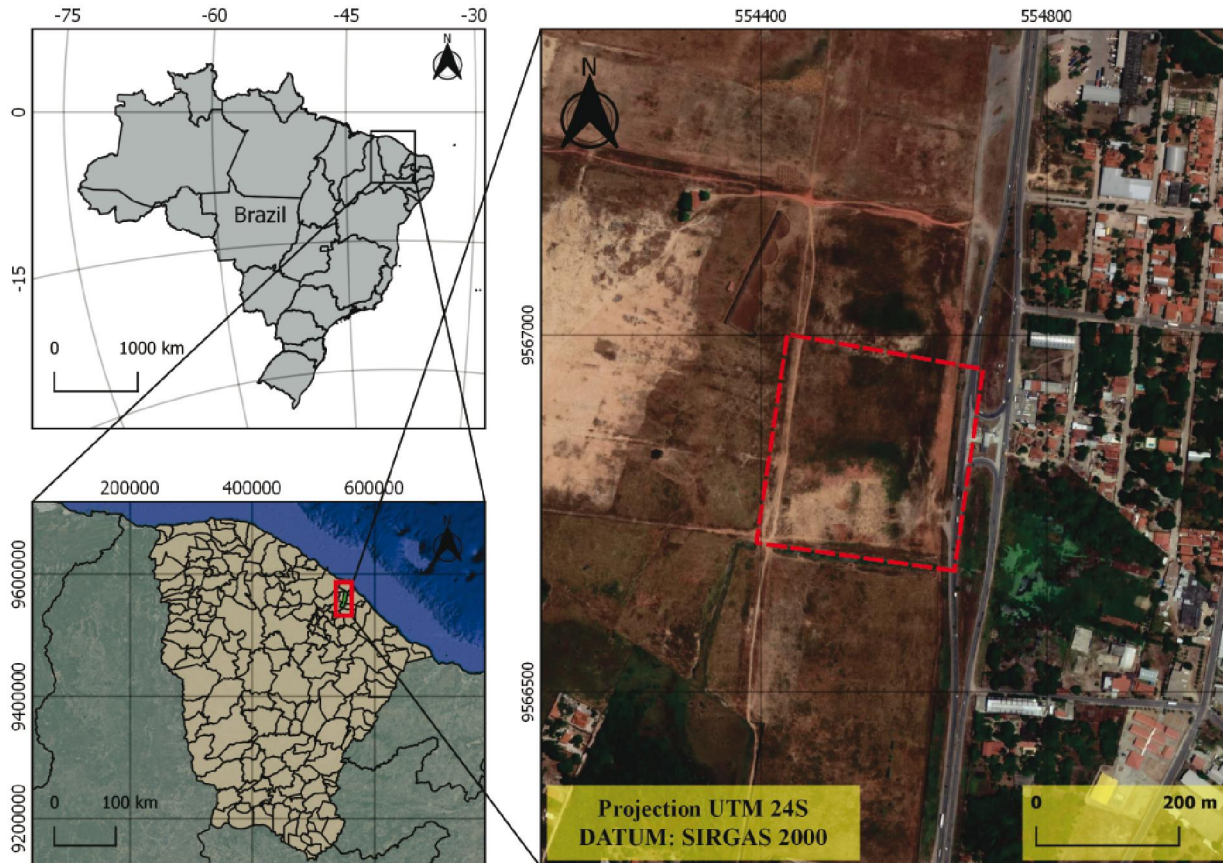
Source: Data from the IBGE (Brazilian Institute of Geography and Statistics) and Google Earth. Prepared by the authors

The area of the flight was determined in the field with the aid of the Ground Station software, where it was possible to automatically program the flight to cover an area of approximately three hectares at a constant speed of 5.0 m s^{-1} and a height of 60 m relative to ground level, generating a GSD (Ground Sampling Distance) of approximately 3.2 cm pixel^{-1}. Upon reaching each vertex in the flight path, the RPA executes a 'Stop and Turn' manoeuvre, which comprises rotating along its own axis before proceeding to the next point. An 80% frontal and 60% lateral overlap was defined.

Fourteen targets (wooden boards) were randomly distributed over the study area to serve as the GCP used in georeferencing the digital model. The coordinates of each control board were obtained with millimetre precision using the Magellan® Pro Mark 3 GNSS system (Figure 2), carrying out a precise point survey and spending 20 minutes on each GCP. Post-processing of the data was carried out by the GNSS Solutions® software, which uses the Brazilian Network for Continuous Monitoring of GNSS

Systems (RBMC) for post-processing and correction of the geographic data.

A computer with a 3.40GHz Intel Core™ i7-3770 processor, 8 GB RAM, and Windows 8 64-bit operating system was used. The PhotoScan software, from AgiSoft, was employed, with processing divided into five stages: 1) importing the aerial images, 2) Aligning the images, 3) Creating the mesh and georeferencing (with eight and five points), 4) Generating the Dense Point Cloud, and 5) Generating the Orthophoto and exporting the reports, as shown in Figure 3. The software also allows texturing of the 3D model, as well as other workflow options.

The aerial images were independently processed in the field using the PhotoScan software with eight, five and three GCP (Ground Control Points), and evaluated against Mapping Accuracy Standards, by calculating the mean squared error of the sample errors. The georeferenced orthomosaic was evaluated based on the points collected using the ProMark 3 GNSS system, as per equations 1, 2, 3 and 4.

Figure 2 - Using the Magellan® Pro Mark3 GNSS system to acquire geographic data of the area in question. The image also shows one of the control boards used

$$e_x = x_t - x_r \tag{1}$$

$$e_y = y_t - y_r \tag{2}$$

where,

e_x = Discrepancy in the x(m) coordinate;

e_y = Discrepancy in the y(m) coordinate;

x_t or y_t = Pixel coordinate in the digital terrain model (m);

x_r or y_r = Coordinate acquired with the GNSS system (Reference) (m).

$$e_{hi} = \sqrt{e_{xi}^2 + e_{yi}^2} \tag{3}$$

where,

e_{hi} = horizontal error component for each point 'i' of the sample (m);

$$RMSE = \sqrt{\frac{\sum_{i=1}^{n} \left(e^2 Hi \right)}{n}} \tag{4}$$

where,

RMSE = root mean square error of the sample (m);

n = Number of samples.
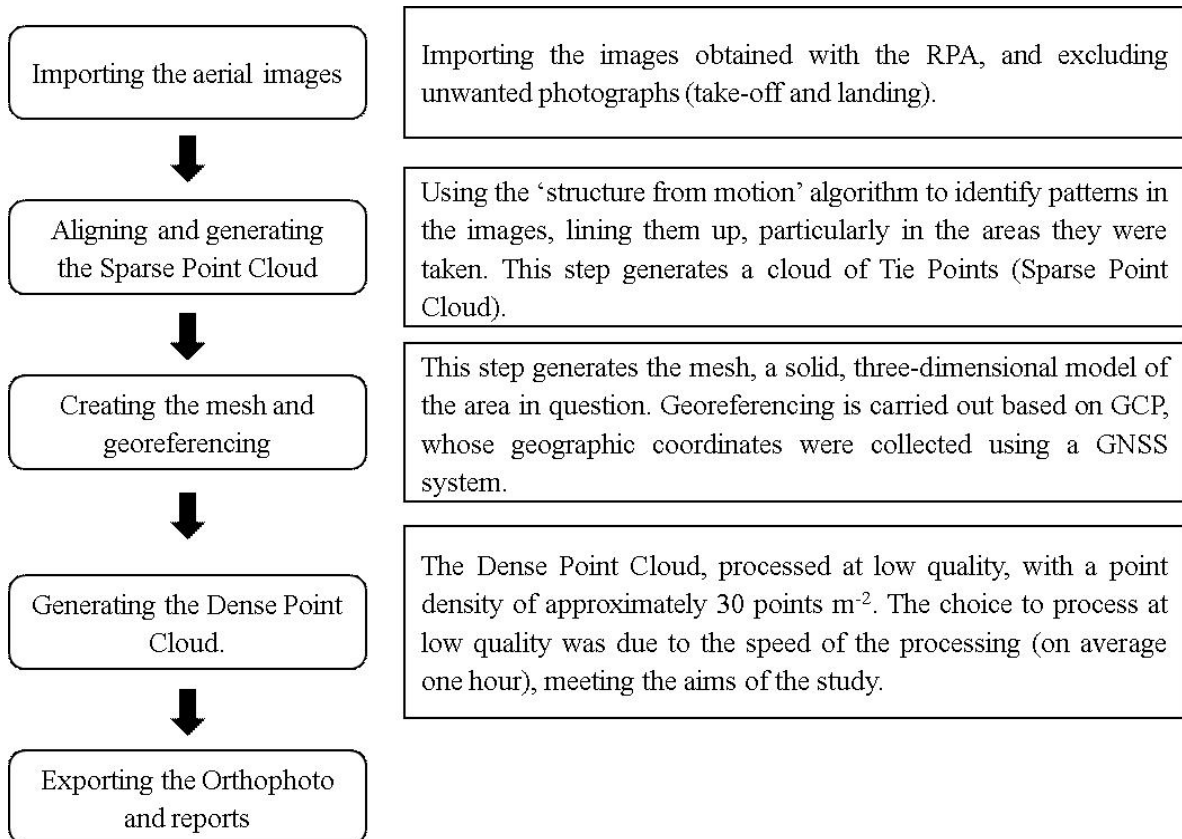
Figure 3 - Workflow using the Agisoft PhotoScan® software

Importing the aerial images	Importing the images obtained with the RPA, and excluding unwanted photographs (take-off and landing).
Aligning and generating the Sparse Point Cloud	Using the 'structure from motion' algorithm to identify patterns in the images, lining them up, particularly in the areas they were taken. This step generates a cloud of Tie Points (Sparse Point Cloud).
Creating the mesh and georeferencing	This step generates the mesh, a solid, three-dimensional model of the area in question. Georeferencing is carried out based on GCP, whose geographic coordinates were collected using a GNSS system.
Generating the Dense Point Cloud.	The Dense Point Cloud, processed at low quality, with a point density of approximately 30 points m^{-2}. The choice to process at low quality was due to the speed of the processing (on average one hour), meeting the aims of the study.
Exporting the Orthophoto and reports	

Table 1 - Mapping accuracy standards for the points used in the production of digital cartographic data

MAS-DMP	1:1000		1:2000		1:5000		1:10000	
	MAS (m)	SE (m)	MAS (m)	SE (m)	MAS (m)	SE (m)	MAS (m)	SE (m)
A	0.28	0.17	0.56	0.34	1.40	0.85	2.80	1.70
B	0.50	0.30	1.00	0.60	2.50	1.50	5.00	3.00
C	0.80	0.50	1.60	1.00	4.00	2.50	8.00	5.00
D	1.00	0.60	2.00	1.20	5.00	3.00	10.00	6.00

MAS - Mapping accuracy standards; DMP - Digital mapping products; SE - Standard Error; Source: Adapted from the Technical Specification Standards for the acquisition of defence geospatial vector data of the ground forces of the Brazilian Army (Version 1.1 - March 2016)

The geometric quality of the cartographic products (orthomosaics) was evaluated using the Mapping Accuracy Standards for Digital Mapping Products (MAS-DMP) established for maps prepared at a scale of 1:1000, where the established acceptable standard planimetric error is 0.28 m for a 'Class A' classification. In order for a digital product to be accepted as a reference for the SCN (National Cartographic System), and consequently for the INDE (National Infrastructure for Spatial Data), the Technical Specification Standards for the Acquisition of Defence Geospatial Vector Data of the Land Forces of the Brazilian Army, establishes that 90% of the errors in the points collected by the cartographic product present values equal to or less than those predicted in the MAS-DMP, when compared to the coordinates surveyed in the field by a high precision method, as shown in Table 1.

Table 1 is crucial for understanding how Brazilian Standards classify digital products, stipulating limits for errors generated in the various processes. As an example, a map with a scale of 1:1000 can have an acceptable error of 0.28 m, while a map with a scale of 1:10000 has an acceptable error of 2.80 m. The statistical analysis, and preparation of the graphs and Statistical Process Control (SPC) maps were carried out using the Excel® and Minitab 16® software.

RESULT AND DISCUSSION

Table 2 shows the horizontal and vertical errors in centimetres when processing with eight, five and three GCP in the X, Y and Z plane, obtained from the error report of the PhotoScan software. Except for the survey using three GCP, the digital products obtained from the aerial images following analysis of the MSE were classified as Mapping Accuracy Standards Class 'A' for a scale of 1:1000. The MSE obtained when processing with three GCP received a 'B' classification.

Carrying out aerial mapping using an RPA has a great advantage, due to the high spatial resolution obtained (ANUROGO *et al.*, 2017; GÓMEZ-CANDÓN; DE CASTRO; LÓPEZ-GRANADOS, 2014). However, the precision achieved in generated digital products, such as the orthophoto and digital elevation models, depends directly on the quality of the GNSS system used, as wel as on the number of control points employed in the process. Conducting surveys with GNSS devices is a task that requires a large amount of time, in addition to mobilising field teams. As such, demonstrating the quality of products generated with a small number of control points (as shown in Table 2) reveals a great advance in mapping using RPA, opening up new possibilities in various areas of geodetics.

Hugenholtz *et al.* (2013), carried out a flight over an area of 4.5 ha seeking to attest to the accuracy of their survey. The authors employed 99 control points, 20 of which were used to quantify horizontal accuracy by RTK GNSS. The RMSE obtained was 0.18 m horizontally and 0.29 m vertically. The study area had areas of dense vegetation, but these had no effect on accuracy, as those responsible for field surveys generally define open and unsheltered areas for placing the GCP. Placing GCP in closed areas makes no sense, since visualising the targets in an aerial image is a basic prerequisite for processing to be viable, it also increases the positioning errors of the GNSS equipment (multi-path effect).

According to Agüera-Vega, Carvajal-Ramírez and Martínez-Carricondo (2017), a minimum of three GCP placed in a triangle are required. However, their results showed that the greater the number of GCP used, the smaller the georeferencing errors and the Mean Squared Error (MSE), corroborating the data presented in Table 2. The authors carried out a survey using RPA, acquiring 160 aerial photographs over 17 hectares at a height of 120 m, with 4, 5, 6 7, 8, 9, 10, 15 and 20 control points. The greatest accuracy was obtained using 15 horizontal GCP, giving values of 0.045 m horizontally and 0.058 m vertically. Despite the survey area being larger, the relief was not very rugged and had little natural vegetation, with several places of exposed soil, similar to the conditions presented in the present article.

Table 2 - Georeferencing errors and Mean Squared Error (MSE) in processing using eight, five and three GCP

GCP	X (cm)	Y (cm)	Z (cm)	Total (cm)	MSE (cm)	MAS
8	3.35305	3.0058	0.44531	4.52505	9.612	A
5	2.86768	5.84235	2.61496	7.01389	15.825	A
3	1.88465	7.45902	3.35552	8.39335	33.825	B

MAS - Mapping Accuracy Standards

Corroborating the results of Zanetti, Gripp Junior and Santos (2017), the number and arrangement of GCP are crucial to the levels of accuracy, directly influencing the quality of the generated products, and considerably increasing the accuracy of the maps. The random and representative distribution of the GCP in the present study was important for achieving the above-mentioned precision. Random and representative distribution is therefore necessary to minimise georeferencing errors.

Another point to be noted is the spatial resolution of the sensor on board the RPA. The RGB camera used in the present study has a resolution of 12 megapixels, generating orthomosaics with a GSD of 3.2 cm pixel^{-1}, which directly favoured manual georeferencing using the PhotoScan software, since the great wealth of mapping detail helped to identify the GCP, minimising human error. Similarly, Bachmann *et al*. (2013), used 40 GCP to calculate the accuracy of thei survey. The mean error obtained in the georeferenced orthomosaic was 0.3 m, greater than the data found in the present study. The explanation may be linked to the resolution of the camera used by Bachmann *et al*. (2013), which had 1.5 megapixels.

In contrast, Gómez-Candón, de Castro and López-Granados (2014) carried out flights at three different altitudes (30, 60 and 100 m above ground level), finding no significant relationship between a decrease in the level of detail and the accuracy of the georeferencing. However, the camera used by the researchers was able to generate a GSD of less than 2.5 cm pixel^{-1} at all altitudes, which must have favoured accurate manual georeferencing of the generated digital products. The researchers found positioning errors of less than 0.03 m. Such accuracy is mainly related to the number of GCP used (11 to 45). However, the authors state that the accuracy of the georeferencing, once reaching a limit of GCP, did not increase significantly as the number of control points increased.

In the present study, when five and eight control points were used, the standard of accuracy was classified as MAS class 'A', which is extremely desirable in mapping. Obviously, distribution of the GCP and accuracy of the GNSS system are crucial factors for obtaining an accuray of less than 0.28 m (limits of MAS class 'A'). For aerial surveys, the advantage of working with a small number of GCP is mainly to do with gaining time. Attesting to the accuracy of digital products opens up a wide range of uses in cartography and topography, meeting the most varied of objectives.

For Brazilian standards, the present study therefore demonstrates methodological advancement, as it attests to the accuracy of mapping using high resolution aerial images processed as orthomosaics. Such evidence leads to the idea of including this technology in various types of topographical and engineering services. Under statistically controlled conditions, the digital products generated by this mapping can provide a new portfolio of services for technicians working in the above areas, resulting in development and income.

When validating positioning, a variation in individual error for each GCP is common (Figure 4), as severl factors are linked to the quality of the georeferencing, such as the time needed for tracking each GCP, the visibility of the GCP in the images, and their distribution in relation to other GCP, in addition to the human error and subjectivity involved in the manual georeferencing process.

Another aspect was the error in identifying the height at ground level. In the present study, processing errors compared to altitude information from the GNSS system were approximately 0.45, 2.61 and 3.36 cm for processing with eight, five and three points respectively, which demonstrates the quality of the Sfm (structure from motion) algorithm in reconstructing a terrain in three dimensions. Zarco-Tejada *et al*. (2014), sought to evaluate the quality of plant-heiht recognition (Olive trees) using aerial images obtained by RPA. The authors attest to a high correlation (R^2 = 0.83) between the data from the point cloud and height measurements in the field, in addition to an estimated altitude error of 0.35 cm, illustrating the great possibilities for precision of reconstructing digital elevation models using RPA.

For the statistical process control, the probability graphs for each of the processes using different control points are shown in Figure 5. In the processes under evaluation, both errors were found to be within the accepted limits, resulting in safe processes from the point of view of individual accuracy. However, as expected, as the number

Figure 4 - Control boards (GCP) in the field used in processing images obtained with RPA (orthophoto). The blue dots represent the projection of the points obtained with the GNSS system in the field. The distance from the blue point to the centre of the plate is shown as the positioning error
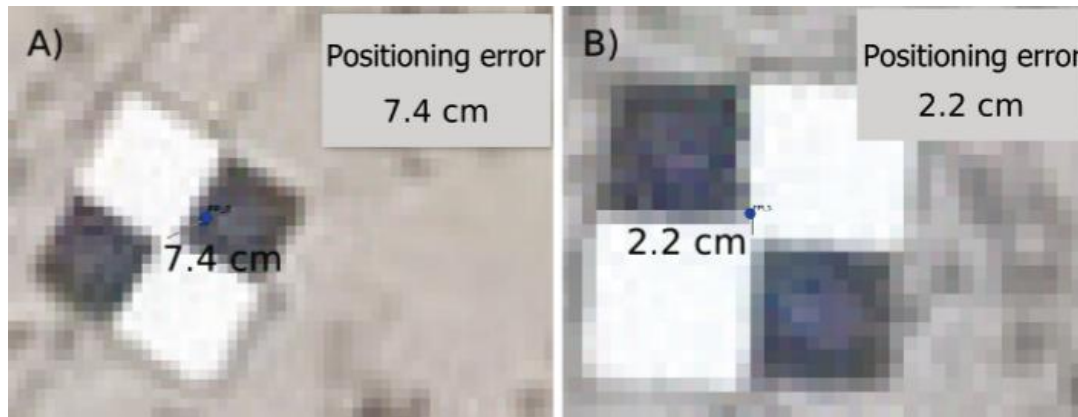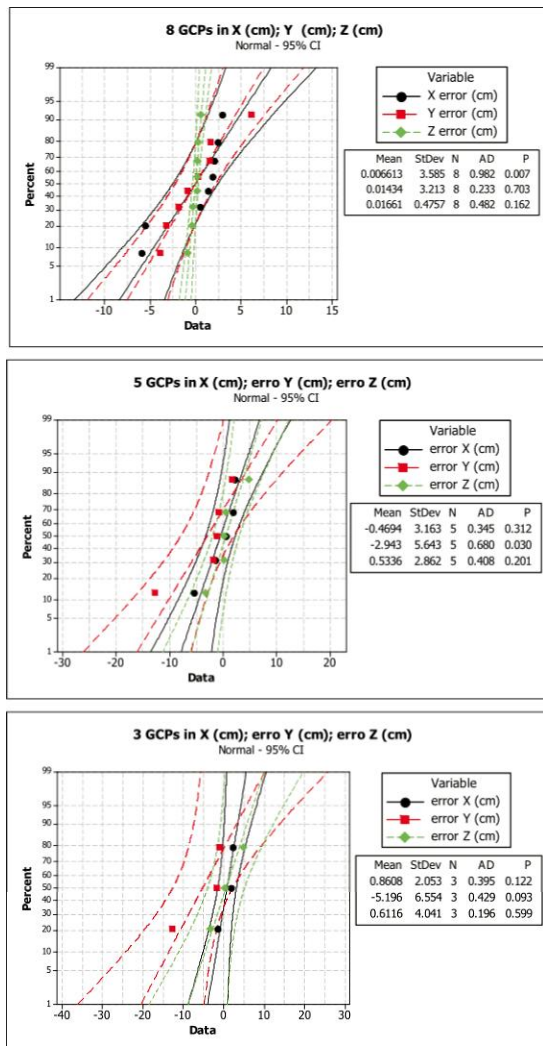

Figure 5 - Probability Tests for errors in processing with eight, five and three GCP


of control points decreases, the natural tendency of the errors is to rise, increasing the inaccuracy of the digital products generated from aerial images obtained via RPA. This agrees with Salvini *et al*. (2018), who related the number and distribution of control points in the area to the statistical accuracy and quality of the mapping products.

The mean value of the errors in X, Y and Z increases as the number of points in the processing is reduced, as shown in Figure 5. In the control maps for processing with three GCP, there is greater range in the errors between sample points. The maps showing the data for the survey carried out with eight GCP have smaller mean errors, which indicates greater control over the variable under analysis. Several studies to assess the quality of these processes are used in the statistical validation of the generated process, as explained by Noronha *et al*. (2011), Takahashi *et al*., (2012) and Silva *et al*., (2013). When mapping using RPA, it is extremely important to check the digital models and attest to their accuracy as a basis for decision making. From a statistical point of view therefore, in surveys of this nature, only five control points (as seen in the present study) are sufficient for mapping to the desired MAS class 'A' and with controlled error processes.

One of the main challenges in placing GCP in the field is accessibility, which is made difficult on uneven terrain and in areas of dense vegetation. Dense vegetation hampers the signal quality of the GNSS equipment, generating the multi-path effect and increasing inaccuracy, in addition to reducing the visibility of the GCP when generating the digital model. In this context, the orthomosaics generated from processing with eight, five and three GCP together with the digital elevation model of the study area are shown in Figure 6.

Figure 6 - Orthomosaics generated from the aerial survey with the RPA: A) with three GCP (ground control points), B) eight GCP, C) five GCP, and D) generated digital elevation model
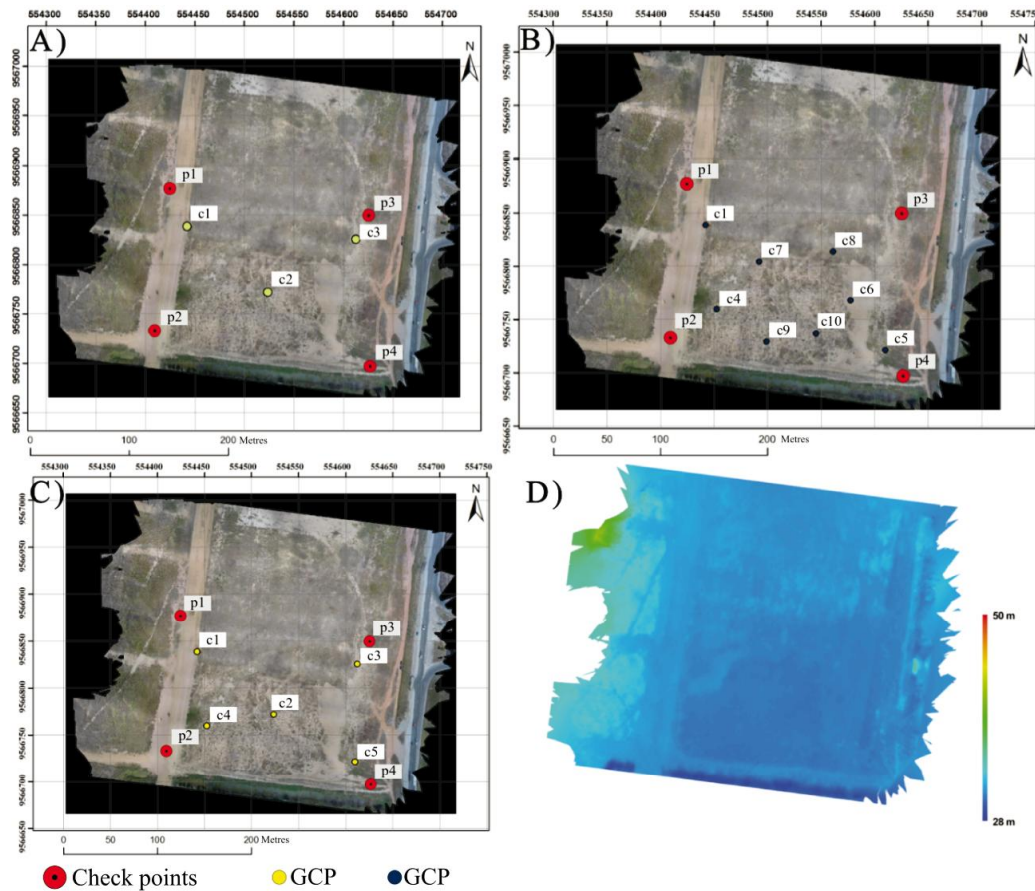
Rugged topography is a physical impediment that can hinder the distribution of GCP in the field, which can have a negative impact on accuracy, since in heavily rugged terrain the mobility of the team involved in the aerial survey is reduced. The study area of the present work has predominantly flat to gently undulating relief, with a mean altitude of 30 metres and low native vegetation, facilitating distribution of the GCP. Other important factors to consider that cause difficulties in placing the GCP, are the presence of water bodies and dense vegetation. The smaller the number of control points used when mapping, the less time spent by the field team, facilitating mapping, and maintaining accuracy within the established standards.

CONCLUSIONS

1. Images obtained with RPA allow products of high cartographic precision to be obtained, which makes it possible to use these tools in mapping, observing the number of GCP and the precision of the GNSS system;

2. Both the horizontal and vertical errors of the Pro Mark 3 GNSS system, and the errors related to the X, Y and Z coordinates of the GCP processed using the PhotoScan software, were within the control limits for the conditions of the study area;

3. Evaluation of the digital products generated from aerial images obtained by means of RPA, using the Mapping Accuracy Standards and the Statistical Control Process, attested to the accuracy of the digital products generated from the aerial survey.

REFERENCES

AGÜERA-VEGA, F.; CARVAJAL-RAMÍREZ, F.; MARTÍNEZ-CARRICONDO, P. Assessment of photogrammetric mapping accuracy based on variation ground control points number using unmanned aerial vehicle. **Measurement**, v. 98, p. 221-227, 2017.

ALSALAM, B. H. Y. *et al*. Autonomous UAV with vision based on-board decision making for remote sensing and precision agriculture. *In*: IEEE AEROSPACE CONFERENCE, 38., 2017, Big Sky. **Proceedings** […]. Big Sky: IEEE, 2017. p. 1-12.

ANUROGO, W. *et al*. A simple aerial photogrammetric mapping system overview and image acquisition using unmanned aerial vehicles (UAVs). **Geospatial Information**, v. 1, n. 1, p. 11-18, 2017.

BACHMANN, F. *et al*. Micro UAV based georeferenced orthophoto generation in vis+ nir for precision agriculture. **International Archives of the Photogrammetry, Remote Sensing and Spatial Information Sciences**, v. 1, p. W2, 2013.

CALOU, V. B. C. *et al*. Estimation of maize biomass using Unmanned Aerial Vehicles. **Engenharia Agrícola**, v. 39, n. 6, p. 744-752, 2019.

FLYNN, K. F.; CHAPRA, S. C. Remote sensing of submerged aquatic vegetation in a shallow non-turbid river using an unmanned aerial vehicle. **Remote Sensing**, v. 6, n. 12, p. 12815-12836, 2014.

FUNDAÇÃO CEARENSE DE METEOROLOGIA E RECURSOS HÍDRICOS. **Dados de pluviometria por faixa de anos - Estado do Ceará**. 2018.

GÓMEZ-CANDÓN, D.; DE CASTRO, A. I.; LÓPEZ-GRANADOS, F. Assessing the accuracy of mosaics from unmanned aerial vehicle (UAV) imagery for precision agriculture purposes in wheat. **Precision Agriculture**, v. 15, n. 1, p. 44-56, 2014.

HUGENHOLTZ, C. H. *et al*. Geomorphological mapping with a small unmanned aircraft system (sUAS): feature detection and accuracy assessment of a photogrammetrically-derived digital terrain model. **Geomorphology**, v. 194, p. 16-24, 2013.

LIMA, R. P. *et al*. The use of RPAS-Remotely Piloted Aircraft Systems in the topographic mapping for mining. **REM-International Engineering Journal**, v. 71, n. 2, p. 281-287, 2018.

MICELI, B. S. *et al*. Avaliação vertical de modelos digitais de elevação (MDEs) em diferentes configurações topográficas para médias e pequenas escalas. **Revista Brasileira de Cartografia**, v. 63, n. 1, 2011.

MONTGOMERY, D. C. **Introdução ao controle estatístico da qualidade**. 4. ed. São Paulo: LTC, 2004. 513 p.

NORONHA, R. H. de F. *et al*. Controle estatístico aplicado ao processo de colheita mecanizada diurna e noturna de cana-de-açúcar. **Bragantia**, v. 70, n. 4, p. 931-938, 2011.

SALVINI, R. *et al*. Use of a remotely piloted aircraft system for hazard assessment in a rocky mining area (Lucca, Italy). **Natural Hazards & Earth System Sciences**, v. 18, n. 1, 2018.

SIEBERT, S.; TEIZER, J. Mobile 3D mapping for surveying earthwork projects using an Unmanned Aerial Vehicle (UAV) system. **Automation in Construction**, v. 41, n. 1, p. 1-14, 2014.

SILVA, R. P. *et al*. Qualidade da colheita mecanizada de feijão (*Phaseolus vulgaris*) em dois sistemas de preparo do solo. **Revista Ciência Agronômica**, v. 44, n. 1, p. 61-69, mar. 2013.

TAKAHASHI, F. H. *et al*. Variação e monitoramento da qualidade do leite através do Controle Estatístico de Processos. **Ciência Animal Brasileira**, v. 13, n. 1, 2012.

TSOUROS, D. C.; BIBI, S.; SARIGIANNIDIS, P. G. A review on UAV-based applications for precision agriculture. **Information**, v. 10, n. 11, p. 349, 2019.

ZANETTI, J.; GRIPP JUNIOR, J.; SANTOS, A. de P. dos. Influence of number and distribution of control points on orthophotos generated from a survey by VANT. **Revista Brasileira de Cartografia**, v. 69, n. 2, p. 263-277, 2017.

ZARCO-TEJADA, P. J. *et al*. Tree height quantification using very high-resolution imagery acquired from an unmanned aerial vehicle (UAV) and automatic 3D photo-reconstruction methods. **European Journal of Agronomy**, v. 55, n. 1, p. 89-99, 2014.